Assessment and Use of NGR Instrumentation on the *JOIDES Resolution* to Quantify U, Th, and K Concentrations in Marine Sediment

by Ann G. Dunlea, Richard W. Murray, Robert N. Harris, Maxim A. Vasiliev, Helen Evans, Arthur J. Spivack, and Steven D'Hondt

doi:10.2204/iodp.sd.15.05.2013

Introduction

Concentrations of uranium (U), thorium (Th), and potassium (K) in geological materials provide insight into many important lithological characteristics and geologic processes. In marine sediment, they can aid in identifying clay compositions, depositional environments, and diagenetic processes. They can also yield information about the alteration and heat production of rocks (Ketcham 1996; Barr et al., 2002; Revillon et al., 2002; Brady et al., 2006; Bartetzko, 2008). Measurements of the concentrations of these elements in geological materials are relatively straightforward in shore-based laboratories. Rapidly determining their abundance within cores of sedimentary and igneous rock sequences onboard a research vessel is a more challenging but potentially very useful method to non-destructively and quickly provide important geochemical information about the concentrations of U, Th, and K within the sequences being cored.

When ^{238}U, ^{232}Th, and ^{40}K radioisotopes decay, they and their daughter products emit gamma rays at specific energy levels unique to each isotope. Natural gamma-ray (NGR) spectroscopy measures a wide energy spectrum that can be used to estimate the abundance of each isotope based on the strength of the signal at characteristic energies (Blum et al., 1997; Gilmore, 2008). Although intensities measured by an NGR system are proportional to the elemental concentrations, converting total counts in the energy spectrum to absolute elemental concentrations can be challenging due to low concentrations in the targeted lithologies and the time constraints of core processing. Measuring ^{238}U, ^{232}Th, and ^{40}K in marine sediment and rock is particularly difficult because certain marine lithologies are commonly an order of magnitude less radioactive than continental material (Kogan et al., 1971; Taylor and McLennan, 1985; Rudnick and Gao, 2003).

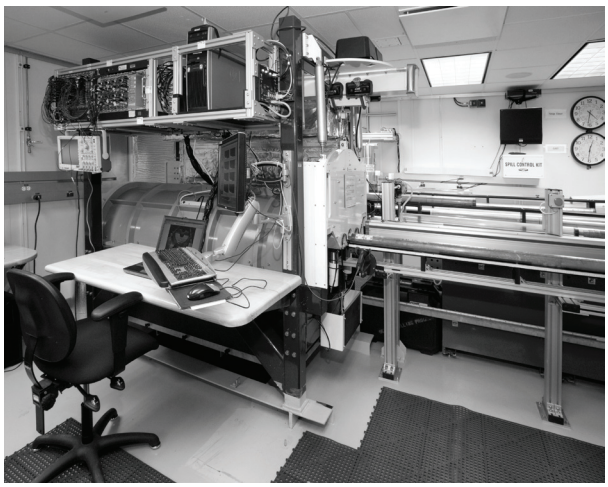

Figure 1. The natural gamma radiation (NGR) system on the *JOIDES Resolution* (from Vasiliev et al., 2011).

Since 1993, an NGR system on the Ocean Drilling Program (ODP)/Integrated Ocean Drilling Program (IODP) drillship *JOIDES Resolution* has successfully been measuring NGR emitted by marine sediment and rocks of varying lithologies (Blum et al., 1997). Additionally, there is a history through Deep Sea Drilling Project (DSDP)/ODP/IODP of downhole logging with NGR tools (Gealy, 1973; Hoppie et al., 1994; Blum et al., 1997; Sakamoto et al., 2003). However, the shipboard NGR system used prior to 2009 often required excessive NGR measurement time in order to produce reliable counting statistics, and hence conflicted with the flow of core processing otherwise imposed by the shipboard operations. Because of their composition in general, deep-sea sediments in particular pose a problem in this regard. This caused the NGR system to be underutilized.

In 2009, a new NGR system was installed on the *JOIDES Resolution* to quicken the pace of NGR measurements while providing the statistical reliability and quality of data needed (Fig. 1, Vasiliev et al., 2011). Now, each core section (up to 1.5 m in length) requires only 10–60 minutes of instrument time to produce a high-resolution energy spectrum. This data from this spectrum can be rapidly converted to concentrations by combining analytical and modeling techniques. Due to instrument design, NGR counts for each set of spectral data are integrated over 40 cm of core length. Vasiliev et al. (2011) details the geometric layout of the improved system and provides an overview of its analytical capabilities, including spatial resolution.

While the new NGR system is a significant step forward, it is important to assess the instrument's performance by comparing NGR-derived results to those from independent measurements. Here we compare the concentrations of U, Th, and K derived from the shipboard NGR instrument to shore-based inductively coupled plasma-mass spectrometer (ICP-MS) and inductively coupled plasma-emission spectrometer (ICP-ES) analyses of 38 samples collected during IODP Expedition 329 to the South Pacific Gyre. The samples are metalliferous pelagic clays and carbonate oozes (D'Hondt et al., 2011). We highlight several simple, yet vital, correc-

tions that must be applied to the raw shipboard NGR data to improve their quality. Our goal is to assess the accuracy and improve the precision of shipboard NGR estimates of U, Th, and K concentrations so future expeditions may more fully use this new NGR system.

NGR Measurements on the *JOIDES Resolution* during Expedition 329

The improved NGR instrument (Vasiliev et al., 2011) was used during IODP Expedition 329. Prior to analyzing each set of sediment core sections, we measured the NGR background spectra for ~5.5 hours to account for cosmic and environmental sources. Twice during the expedition, we calibrated each NaI(Tl) detector using a set of 1-mkCi ^{137}Cs and ^{60}Co gamma-ray calibration sources. Measurements of cylindrical core-shaped standards with known abundances of ^{40}K allowed us to convert NGR counts per second (cps) to concentrations of total K, assuming natural abundances of K isotopes. We obtained the NGR data reported in this study (Table 1) by measuring the energy spectrum emitted by each core section (1.5 m maximum) for 60 minutes. Additional information is described by D'Hondt et al. (2011).

The decay of ^{40}K to ^{40}Ar produces a distinct peak at 1460 keV on the NGR spectrum. ^{238}U and ^{232}Th do not emit detectable gamma rays when they decay, but some of their daughter products emit a gamma-ray energy signal that is apparent in the measured spectrum. We used the daughter products with the most obvious energy signal, ^{214}Bi (1.76 MeV) and ^{208}Tl (2614 keV) to indicate the presence of the parent isotopes ^{238}U and ^{232}Th, respectively (Kogan,

Table 1. Concentrations of U, Th, and K from the ICP-MS, ICP-ES, and NGR measurements.

Site/ Hole	Depth (mbsf)	K ICP-ES Not Normalized wt%	K ICP-ES Normalized wt%	Th ICP-MS ppm	U ICP-MS ppm	K NGR Uncorrected wt%	Th NGR Uncorrected ppm	U NGR Uncorrected ppm	Bulk/Dry MAD Density	K NGR Corrected %	Th NGR Corrected ppm	U NGR Corrected ppm
1366B	0.1	2.27	2.85	16.00	1.66	0.75	2.80	0.90	3.32	2.49	9.31	2.99
	1.8	2.43	2.88	15.56	1.94	0.96	4.80	1.60	3.32	3.19	15.95	5.32
	3.5	2.65	3.16	14.70	1.93	0.97	2.80	0.80	3.32	3.22	9.31	2.66
	5.1	2.71	3.25	12.09	1.94	1.28	6.00	1.50	3.32	4.25	19.94	4.99
	6.2	2.66	3.29	13.33	2.30	0.98	4.80	1.70	3.32	3.26	15.95	5.65
	7.9	1.60	2.18	12.92	2.77	0.63	3.50	1.20	3.32	2.09	11.63	3.99
	10.1	1.91	2.42	17.64	3.81	0.87	6.40	1.20	3.32	2.89	21.27	3.99
	13.1	2.58	3.45	5.59	2.33	1.25	2.20	1.60	2.36	2.95	5.19	3.78
	15.8	3.01	3.67	3.79	20.4	1.43	1.80	1.50	2.36	3.38	4.25	3.54
1367B	0.2	1.99	2.58	15.90	3.87	1.43	6.00	20.40	2.78	3.97	16.67	56.66
	1.2	1.94	2.54	7.93	3.85	0.92	2.50	1.60	2.78	2.56	6.94	4.44
	1.8	2.02	2.64	7.56	3.81	1.14	3.10	2.90	2.78	3.17	8.61	8.05
	3.3	2.17	2.74	7.77	3.87	1.05	2.90	2.60	2.78	2.92	8.05	7.22
	6.5	0.08	0.26	0.43	0.29	0.69	2.60	2.90	1.63	1.12	4.24	4.73
	7.2	0.08	0.24	0.43	0.37	0.15	0.60	0.60	1.63	0.24	0.98	0.98
	7.7	0.21	0.45	1.41	1.81	0.12	0.50	0.90	1.63	0.20	0.82	1.47
	12.1	0.05	0.14	0.15	0.60	0.05	0.30	0.60	1.63	0.08	0.49	0.98
	17.1	0.06	0.16	0.08	1.15	0.08	0.20	1.20	1.63	0.13	0.33	1.96
	21.5	0.16	0.46	0.05	0.79	0.09	0.20	1.20	1.63	0.15	0.33	1.96
1368B	0.2	0.23	0.56	2.04	1.26	0.10	0.25	3.33	1.82	0.18	0.46	6.08
	0.5	0.08	0.25	0.37	0.85	0.10	0.25	1.33	1.82	0.18	0.46	2.43
	2.6	0.06	0.17	0.07	0.94	0.07	0.20	0.93	1.82	0.13	0.36	1.70
	3.9	0.06	0.18	0.12	0.50	0.04	0.11	0.44	1.82	0.07	0.20	0.80
	6.3	0.06	0.15	0.05	0.99	0.04	0.20	0.48	1.82	0.07	0.36	0.88
	8.2	0.05	0.15	0.03	0.71	0.01	0.03	0.07	1.82	0.02	0.05	0.13
	10.5	0.06	0.15	0.04	1.39	0.06	0.15	0.72	1.82	0.11	0.27	1.31
	11.2	0.07	0.17	0.08	2.56	0.09	0.23	1.11	1.82	0.16	0.42	2.03
	12.9	0.09	0.20	0.07	1.97	0.09	0.21	1.01	1.82	0.16	0.38	1.84
	15.3	0.55	0.58	1.36	0.91	0.25	0.36	1.85	1.82	0.46	0.66	3.38
1369B	0.2	2.35	2.85	14.27	1.61	1.31	9.70	32.80	3.42	4.48	33.15	112.11
	2.8	2.68	3.24	11.99	1.38	1.05	3.90	1.31	3.42	3.59	13.33	4.48
	3.3	2.99	3.63	12.11	1.47	1.22	4.50	1.01	3.42	4.17	15.38	3.45
	5.6	2.70	3.32	16.07	1.96	1.01	3.75	1.01	3.42	3.45	12.82	3.45
	7.2	3.20	3.74	13.82	1.81	1.85	5.93	1.54	2.48	4.58	14.69	3.81
	8.8	2.79	3.31	17.01	2.45	1.16	5.10	1.45	2.48	2.87	12.63	3.59
	11.3	3.12	3.72	12.97	2.24	1.83	5.49	1.83	2.48	4.53	13.60	4.53
	14.1	3.43	4.11	11.92	2.44	1.99	7.37	1.65	2.48	4.93	18.26	4.09
	16.5	3.24	3.91	12.66	2.56	1.59	4.78	1.07	2.48	3.94	11.84	2.65

The freeze-dried concentrations of major oxides determined by ICP-ES were normalized to 100% to represent dry, volatile-free concentrations of K to better compare with concentrations from samples dried in a convective oven (see text). Column 3 reports the freeze-dried ICP-ES K (wt%, measured at λ=766.490nm) concentrations prior to normalization, and column 4 reports the normalized K (wt%) concentrations. Columns 7–9 report the raw NGR estimates of U, Th, and K concentrations. Column 10 reports the bulk density to dry density ratio from the MAD data that was used to correct the NGR data from wet concentration to dry concentrations. There was limited moisture and density (MAD) data that was co-located with our samples, so we averaged the density data from similar samples at each site that showed a consistent gamma-ray attenuation (GRA) density. Columns 11–13 report the density-corrected NGR results.

1971). By measuring decays of daughter products as a proxy for ^{238}U and ^{232}Th concentrations, it is assumed that the analyzed sediment is in a state of secular equilibrium. However, this assumption is not always valid, as discussed below.

For each NGR-measured ^{40}K peak, we converted the area under the background-corrected spectral peak (Vasiliev et al., 2011) to concentrations based on the cps/concentration ratio of a K standard (with natural abundances of K isotopes) and the mass of the sediment that contributed to the radiation received by each NaI detector. Each detector receives radiation from ~20 cm of core on either side of the detector, and thus all NGR measurements are integrated over ~40 cm (Vasiliev et al., 2011).

The mass of sediment is determined by convolving the NGR detector response function with core densities and core volumes. The "core volume" term in the calculation is the volume of the cylindrical K standard in the visible range of the NaI detector, where core densities are measured with the shipboard gamma-ray attenuation (GRA) system. The statistical error of GRA densities is estimated to be less than 0.5%, and errors in accuracy are less than 5% (Blum, 1997). The error in the GRA density combined with statistical counting and systematic error for the NGR measurements is estimated to be ~7%–8% for K.

For much marine sediment, including those we describe here from the South Pacific Gyre, U and Th cannot be calibrated by simple comparison to a standard because the concentrations are too low given a reasonable measurement time, and the dynamic range of available standard reference materials is too narrow. Instead, we estimated U/K and Th/K ratios by comparing the measured NGR spectra to spectra generated by Monte Carlo simulations (Sambridge and Mosegaard, 2002).

The Monte Carlo simulations were performed on the *JOIDES Resolution* using the GEANT 3.21 simulation tool designed at CERN (Brun et al., 1994; Vasiliev et al., 2011). A single Monte Carlo-simulated spectrum that was generated using a unique combination of ^{238}U, ^{232}Th, and ^{40}K activity ratios will best match the experimentally measured spectrum and reveal the U/K and Th/K ratios. The concentrations of U and Th can then be calculated by multiplying these ratios by the concentrations of K determined from the calibration standard. The spectral analysis for the NGR system that computes elemental concentrations for U, Th, and K are based on natural abundances of the isotopes ^{238}U, ^{232}Th, and ^{40}K (Vasiliev et al., 2011). The statistical error for the Monte Carlo simulations is negligible, but systematic errors are ~10% and in many cases may be much lower.

ICP-MS and ICP-ES Quantification of U, Th, and K Concentrations

To assess the accuracy of the U, Th, and K concentrations generated from the shipboard NGR, we selected 38 samples from discrete depth intervals from Holes U1366B, U1367B, U1368B, and U1369B (Table 1). We used well-established ICP-MS and ICP-ES methods to determine accurate and precise concentrations of these 38 samples (Murray and Leinen, 1996; Martinez et al., 2007; Ziegler et al., 2007). We freeze-dried, powdered, and digested the samples in a sealed heated acid cocktail containing HNO_3, HCl, HF, and H_2O_2. Additions of boric acid after the initial digestion neutralized the HF. We analyzed the solutions at Boston University on a VG PlasmaQuad Excell ICP-MS for U and Th concentrations, and on a Jobin Yvon Ultima C ICP-ES for K concentrations. Based on replicate analysis from the powder weighing step onward, the precision of the K measurement is 4% of the measured value, and the precision of both U and Th is 2% of their respective measured values. To ensure accuracy, we analyzed the BHVO-2 Standard Reference Material (Wilson, 1997; U.S. Geological Survey) independent from our calibrations. Our measured values agree with the reported values (and their reported uncertainty) within analytical precision. Because of this high precision and accuracy, in our discussion we consider the ICP-MS and ICP-ES data (Table 1) to be the benchmark against which we assess the NGR results.

Importance of Accurate Sediment Density Measurements

Sediment density is a critical parameter when comparing U, Th, and K concentrations from NGR measurements to ICP-MS and ICP-ES methods. The concentrations derived from NGR are based on a GRA density, which represents a bulk, *wet* density. In contrast, the ICP-MS and ICP-ES analyses require that the samples be freeze-dried before dissolution, and thus the ICP-MS and ICP-ES data are a concentration based on a *dry* sample weight. Therefore, a density correction (wet to dry) is required prior to comparing shipboard NGR-based concentrations to shore-based ICP-MS and ICP-ES concentrations. This density correction is theoretically straightforward, but in reality there are a number of different parameters that need to be considered throughout the density correction process due to the density measurement techniques, the physical nature of core material, and other aspects of NGR analysis.

We took advantage of the moisture and density (MAD) data collected during Exp. 329 to determine the bulk wet density/dry bulk density ratio (ρ_{bulk}/ρ_{dry}) and to correct the NGR-based measurements for direct comparison with the ICP-ES based concentrations according to the following relationship:

$$[K(wt\%)_{ICP\text{-}ES}] = (\rho_{bulk} / \rho_{dry})[K(wt\%)_{NGR}].$$

Different methods of drying sediment can lead to disparities between data sets. Following typical standard protocol, the Exp. 329 shipboard scientific party measured the wet and dry sediment densities by weighing ~7 cm^3 of wet sediment, drying the sample in a convection oven at 105°C ± 5°C for more than 24 hours, cooling it in a desiccator, and then reweighing it to determine the MAD bulk and dry densities.

The accuracy and precision of the MAD masses determined on the *JOIDES Resolution* while at sea are both stat-ed to be ~0.1% (Blum, 1997), which are likely to be low estimates.

Baking the sediment in a convective oven to measure dry density (ρ_{dry}) removes an undetermined amount of the interlayer water from clay minerals and also potentially drives off some CO_2 from carbonates, regardless of mineralogy. However, freeze-drying the sediment for ICP-MS and ICP-ES analyses retains the interlayer water and CO_2. Therefore, the dry weights on which the ICP-MS and ICP-ES concentrations are based are different from the dry weights on which the NGR calcula-tions are based, even after the ρ_{bulk}/ρ_{dry} correction is employed. This difference can be fairly substantial, yet variable depending on sediment composition.

To account for this weight difference, we determined the concentrations of all ten major element oxides in the sediment using the ICP-ES and normalized the oxides (including K_2O) to sum to 100%. Calculating this "volatile-free" ICP-ES data yields the most appropriate K_2O data to compare to the density-corrected NGR data. Performing this correction is important not only for comparing NGR and ICP measurements in our study, but is also critical to consider when using NGR data as a scientific data set; because the NGR data taken alone at face value is based on a *wet* measurement, comparison to literature data may not be straightforward. It also means that in order to effectively calibrate the NGR to shore-based analyses of K, *all* major oxides need to be analyzed even if K is the only element of scientific interest to a particular investigator.

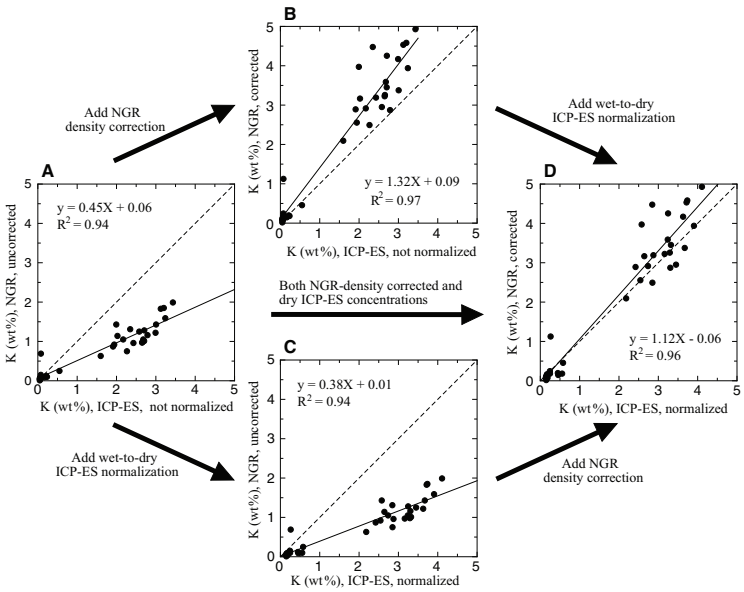

Figure 2. ICP-ES vs. NGR concentrations of K wt% for 38 samples from 4 holes in the South Pacific Gyre. [A] Raw data before the NGR data was density corrected and before the ICP-ES data were normalized to anhydrous values. [B] The K wt% correlation plot after the NGR estimates have been density corrected, but without the normalization of ICP-ES concentrations. [C] The normalized ICP-ES concentrations of K wt% plotted against the NGR data that have not been density corrected. [D] The final results correlating normalized ICP-ES concentrations of K wt% with the density-corrected NGR estimates of K wt%.

Comparison of NGR Data with ICP-MS and ICP-ES Data

The complete raw data generated from shipboard NGR measurements and shore-based ICP-ES and ICP-MS analyses are presented in Table 1. We discuss our K results first because the U and Th data are based on the K concentrations in the NGR measurements (see previous section). Figure 2 illustrates the combined significance of the density correction and use of anhydrous ICP-ES concentrations. Prior to any correction, comparing the raw shipboard-produced NGR data to the non-normalized ICP-ES data (Fig. 2a) shows that the NGR data is offset significantly from the ICP-ES data. The correlation between the data is strong (R^2=0.94), yet the raw NGR values are approximately one-half of the ICP-ES concentrations (slope=0.45). Performing the density correction alone (Fig. 2b) slightly improves the correlation (R^2=0.97) but causes the NGR estimates to be ~30% higher than the ICP-ES concentrations (slope=1.32). Performing the anhydrous correction to ICP-ES data without the density correction (Fig. 2c) causes the NGR results to underestimate ICP-ES concentrations, decreasing the accuracy (slope=0.38) but leaving the correlation unchanged (R^2=0.94). Application of *both* the density correction and the anhydrous correction (Fig. 2d) results in the best comparison between datasets (slope=1.12) and essentially retains the best correlation (R^2=0.96).

While seemingly straightforward, the density measurements themselves also contain nuances that affect the data (Blum, 1997) and are the likely cause of the 1.12 slope value. Since we use the MAD bulk density and dry density as a ratio in Equation 1, any errors in the bulk volume measurement arithmetically cancel and do not affect the results. However, the GRA bulk densities used in converting NGR cps to concentrations can be skewed toward lower values by fractures, gaps, or expansion/compression in the sediment cores that result from pressure changes, mechanical stretching, gas escaping, or other disturbances during the coring process. Additionally, the gamma-ray attenuation (GRA) measurements assume that the average attenuation coefficient is constant for the measured material, which may not be the case if the characteristics of the sediment core vary (Blum, 1997). These factors, coupled with the fact that MAD and NGR data are not always co-located, contribute to the observed scatter between the NGR and ICP-ES data for K.

Additional sources of error may originate from the differences in sampling resolution between the NGR system and ICP-MS and ICP-ES analyses. As noted previously, the NGR measurements integrate over ~40 cm of core length (Vasiliev et al., 2011). In this study, the ICP-MS and ICP-ES methods sampled over 10-cm intervals. The different resolutions

alone may produce error of up to 5%–10% between the two data sets, with stratigraphic lithological contrasts being smeared in the NGR data. Contrasts in lithology, either within one site or between the sites, may also influence the scatter.

Thus, there are a number of factors contributing to the inconsistencies between the NGR and ICP data. Because we calculate the NGR-based U and Th data from the ratio to K concentrations, the scatter within the K dataset will propagate through to the U and Th data as well (Fig. 3). Comparisons between our NGR and ICP-MS values of Th reveal good accuracy (slope=1.05) but a degraded correlation (R^2=0.87) relative to the K comparison. U comparisons show less accuracy (slope=1.20) and a poorer correlation (R^2=0.67) between the datasets. We further note that the U comparative plot is the only one that has a significant y-intercept (Fig. 3). This may reflect the impacts of secular disequilibrium, as described in the next section, or merely that U is the lowest concentration element of the three measured by NGR and thus may be expected to be the least precise.

U-Series Secular Disequilibrium

Several samples from shallow depths in the cores show large disparities between NGR and ICP-MS concentrations of U, which we interpret as indicating that the system is not in secular equilibrium. This trend arises from the difference in chemical properties of ^{238}U and ^{230}Th in seawater and manifests itself in our data because of the inherent differences between what each technique measures. ICP-MS measures ^{238}U directly, while NGR *infers* ^{238}U concentrations by measuring the decay of ^{214}Bi, its daughter product.

A system is in secular equilibrium when the concentration of each radioactive isotope in a decay chain series is solely dictated by the amount of decay of its parent isotope (Faure and Mensing, 2004). Over time, an isolated radioactive system will approach secular equilibrium, typically taking about six times the half-life of the longest-lived daughter to fully equilibrate (Bourdon et al., 2003). Thus, the ^{238}U- and ^{232}Th-decay series require approximately 1.5 Myr and 40 years, respectively, to reach secular equilibrium.

The equilibration process is disrupted if there is a separation between parent and daughter isotopes in the system, which commonly occurs between U and Th in seawater. When ^{238}U dissolved in seawater eventually decays to ^{230}Th, the ^{230}Th daughter product is rapidly scavenged and deposited on the seafloor (Bacon, 1984). Thus, the surface of the seafloor becomes enriched in ^{230}Th and subsequent daughter products relative to the concentration of the ^{238}U parent present. At the seafloor, the initial system is not in secular equilibrium, but as time passes and the sediment is buried, the system approaches a state of equilibrium.

The most shallowly buried samples analyzed in this study in Holes U1367B, U1368B, and U1369B show significantly higher U concentrations estimated from NGR than from ICP-MS (Fig. 4). We interpret that this difference results from the excess of ^{238}U-decay daughter products on the seafloor and can be measured by NGR spectroscopy before the system has reached secular equilibrium. In contrast, ICP-MS analysis of ^{238}U only measures the parent product (and not the daughter products) and thus more accurately quantifies U concentrations in samples that are not at secular equilibrium. Our interpretation is supported by the complete NGR profiles from Exp. 329 (D'Hondt et al., 2011) that show a more gradual decline in ^{214}Bi gamma radiation deeper down each hole.

Sedimentation rates in the South Pacific Gyre are on the order of 0.1–1 m Myr^{-1} (Expedition 329 Scientists, 2011) and consequently, the sediment reaches secular equilibrium in less than 1.5 meters below the seafloor. NGR measurements of sediment from other regions with higher sedimentation rates may give the appearance that ^{238}U and ^{232}Th concentrations decline over a greater depth below the seafloor. For example, during the Pacific Equatorial Age Transect (PEAT) IODP expeditions (Pälike et al., 2010), the NGR system measured high concentrations of ^{238}U-series isotopes near the seafloor, due to the enrichment in the daughter product ^{230}Th, and exponentially decayed to a low concentration at depth as secular equilibrium was achieved (T. Williams, G. Winckler, and M. Lyle, pers. comm., 2012; Williams and Winckler, 2012).

Considerations for Future Applications

Our study shows that after employing the various corrections, use of the NGR/Monte Carlo technique onboard the *JOIDES Resolution* has the potential to rapidly determine U, Th, and K concentrations in marine sedimentary sequences, and thus contribute to the successful achievement of drilling objectives.

The accuracy and precision of the required NGR density corrections, however, depends on the accuracy and precision of both the wet and dry weight measurements. Accurate characterization of the wet vs. dry density in core materials is therefore essential to ensure the accuracy of U, Th, and K concentrations determined from the NGR measurements.

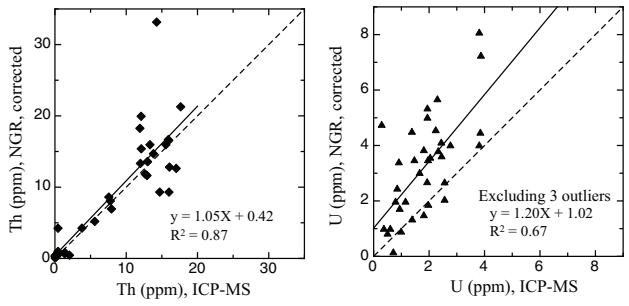

Figure 3. Total U and Th concentrations measured by ICP-MS vs. density-corrected U and Th concentrations measured by NGR for the 38 samples from 4 sites in the South Pacific Gyre that were analyzed for this study. Three outliers were removed from the U graph and are discussed in the section about secular disequilibrium.

One methodological improvement in this regard would be to dry sediment for MAD data on the *JOIDES Resolution* using a freeze-drier rather than a convection oven. Indeed, this was originally suggested by Blum (1997) and would eliminate the need for the anhydrous correction shown in Fig. 2c.

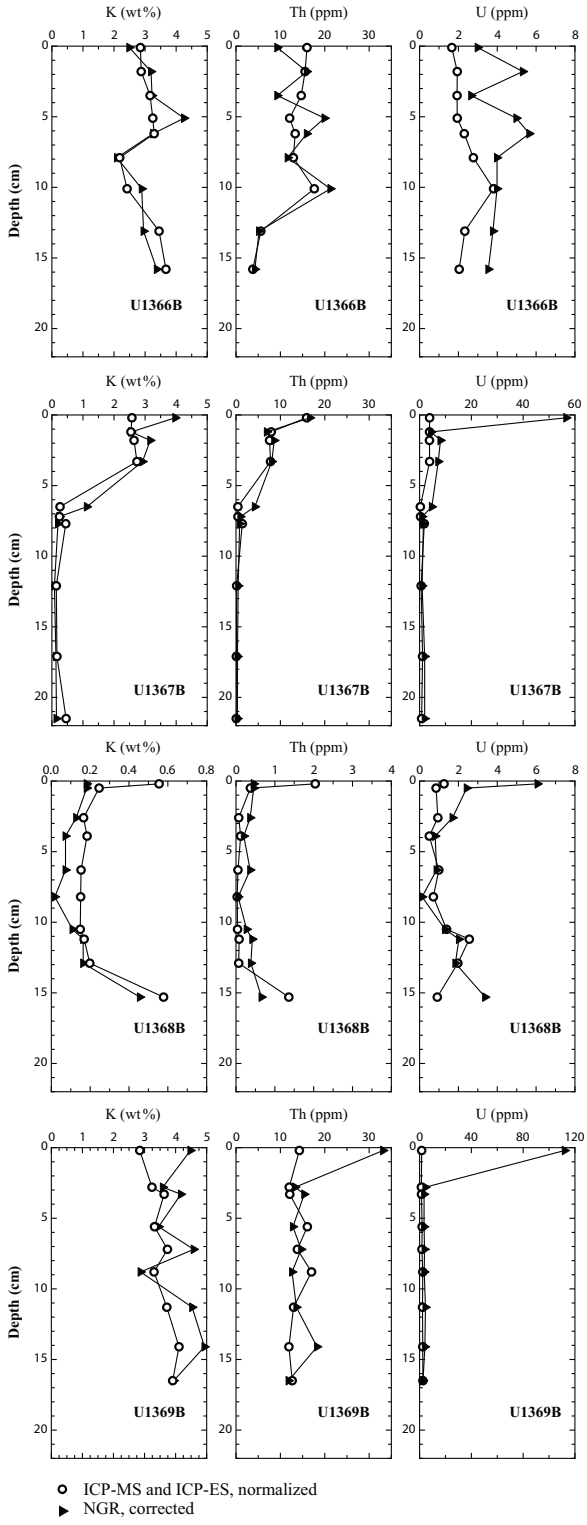

Figure 4. Depth profiles of the concentrations of K, Th, and U for Holes U1366B, U1367B, U1368B, and U1369B showing ICP-MS and ICP-ES data (circles) and NGR density-corrected data (triangles). Additional NGR total cps data from Expedition 329 (not shown here) illustrates a more continuous equilibration trend from the highest NGR emitted from sediment at the sediment-water interface and declining with depth.

Reported values should fully describe how density was measured.

Quantifying the wet to dry density ratio should be done as precisely as possible for a variety of samples from different lithologies throughout the sediment sequence that is being analyzed for NGR to reduce scatter produced by different lithologies and their transitional boundaries. Additionally, the shipboard ICP-ES could be used to quantify concentrations of elemental K in the core material, thereby checking the NGR system's accuracy while at sea. If the ICP samples are freeze-dried and the NGR samples continue to be oven-dried, then all ten major elements will need to be determined by ICP in order to facilitate the anhydrous-based data conversion. When incorporating the various data sets (GRA, MAD, NGR, ICP-ES and/or ICP-MS), samples must be co-located when possible to further enhance appropriate application of the density and anhydrous corrections.

Secular disequilibrium in young marine sediment near the seafloor should also be considered when determining the U and Th concentrations with the NGR system because it measures the daughter products of ^{238}U and ^{232}Th instead of the parent isotope. In the South Pacific Gyre, slow sedimentation rates cause the upper several decimeters of sediment cores from three sites to be in ^{238}U-series secular disequilibrium, while the ^{232}Th-series appears to be fully equilibrated throughout the sediment column.

Acknowledgements

We are grateful to T. Ireland, J. W. Sparks, and R. P. Scudder at Boston University for their analytical assistance, as well as the TAMU scientific support staff on the *JOIDES Resolution* for their assistance during the expedition. We thank an anonymous reviewer for their helpful suggestions, and particularly IODP Data and Publications Manager Jamus Collier for his thoughtful handling of this paper. We also thank T. Williams, M. Lyle, and G. Winckler for helpfully educational conversations. This research used samples and/or data provided by the IODP. Funding for this research was provided by USAC post-cruise support to Expedition 329 shipboard participants R. W. Murray, R. N. Harris, S. D'Hondt, H. Evans, and A. J. Spivack.

References

Bacon, M. P., 1984. Glacial to interglacial changes in carbonate and clay sedimentation in the Atlantic Ocean estimated from ^{230}Th measurements. *Chem. Geol.*, 46(2):97–111. doi:10.1016/0009-2541(84)90183-9

Barr, S. R., Revillon, S., Brewer, T. S., Harvey, P. K., and Tarney, J., 2002. Determining the inputs to the Mariana Subduction Factory: Using core-log integration to reconstruct basement lithology at ODP Hole 801C. *Geochem. Geophys. Geosyst.*, 3(11):8901. doi:10.1029/2001GC000255

Bartetzko, A., 2008. Gamma ray spectrometric analysis of hydrothermally altered dacite samples from the PACMANUS hydrothermal field: Implications for the interpretation of gamma ray wireline measurements. *J. Volcanol. Geotherm. Res.*,

175(3):269–277. doi:10.1016/j.jvolgeores.2008.03.014

Blum, P., 1997. Physical properties handbook. *ODP Tech. Note*, 26. doi:10.2973/odp.tn.26.1997

Blum, P., Rabaute, A., Gaudon, P., and Allan, J. F., 1997. Analysis of natural gamma-ray spectra obtained from sediment cores with the shipboard scintillation detector of the Ocean Drilling Program: Example from Leg 156. *In* Shipley, T. H., Ogawa, Y., Blum, P., and Bahr, J. M., *Proc. ODP, Sci. Results,* 156: College Station, TX (Ocean Drilling Program), 183–195.

Bourdon, B., Turner, S., Henderson, G. M., and Lundstrom, C. C., 2003. Introduction to U-series geochemistry. *Rev. Mineral. Geochem.*, 52:1–21. doi:10.2113/0520001

Brady, R., Ducea, M., Kidder, S., and Saleeby, J., 2006. The distribution of radiogenic heat production as a function of depth in the Sierra Nevada Batholith, California. *Lithos*, 86(3–4):229–244. doi:10.1016/j.lithos.2005.06.003

Brun, R., Bruyant, F., and Marie, M., 1994. GEANT – Detector Description and Simulation Tool. CERN Program Library Long Writeup W5013, CERN, Geneva, Switzerland.

D'Hondt, S., Inagaki, F., Alvarez Zarikian, C. A., and the Expedition 329 Scientists, 2011. *Proc. IODP,* 329: Washington, DC (Integrated Ocean Drilling Program Management International, Inc.). doi:10.2204/iodp.proc.329.2011

Expedition 329 Scientists, 2011. South Pacific Gyre subseafloor life. *IODP Prel. Rept.,* 329. doi:10.2204/iodp.pr.329.2011

Faure, G., and Mensing, T. M., 2004. *Isotopes: Principles and Applications* (3rd ed.): Hoboken (John Wiley & Sons).

Gealy, E. L., 1973. Natural gamma radiation of sediments from the Western Equatorial Pacific: Leg 7, *Glomar Challenger. In* Winterer, E. L., et al., *Init. Repts. DSDP*, 7: Washington, DC (U.S. Government Printing Office), 1037–1080. doi:10.2973/dsdp.proc.7.123.1971

Gilmore, G., 2008. *Practical Gamma-Ray Spectrometry* (2nd ed.): Hoboken (John Wiley & Sons). doi:10.1002/9780470861981

Hoppie, B., Blum, P., and Party, S. S., 1994. Natural gamma-ray measurements on ODP cores: Introduction to procedures with examples from Leg 150. *In* Mountain, G. S., Miller, K. G., Blum, P., et al., *Proc. ODP, Init. Repts.*, 150: College Station, TX (Ocean Drilling Program), 51–59.

Ketcham, R. A., 1996. Distribution of heat-producing elements in the upper and middle crust of southern and west central Arizona: Evidence from the core complexes. *J. Geophys. Res.*, 101(B6):13611–13632.

Kogan, R. M., Nazarov, I. M., and Fridman, Sh. D., 1971. Gamma spectrometry of natural environments and formations: Theory of the method applications to geology and geophysics. Israel Program for Scientific Translations (Jerusalem), No. 5778. Translated from Russian.

Martinez, N. C., Murray, R. W., Thunell, R. C., Peterson, L. C., Muller-Karger, F., Astor, Y., and Varela, R., 2007. Modern climate forcing of terrigenous deposition in the tropics (Cariaco Basin, Venezuela). *Earth Planet. Sci. Lett.*, 264:438–451. doi:10.1016/j.epsl.2007.10.002

Murray, R.W., and Leinen, M., 1996. Scavenged excess aluminum and its relationship to bulk titanium in biogenic sediment from the central equatorial Pacific Ocean. *Geochim. Cosmochim. Acta*, 60(20):3869–3878. doi:10.1016/0016-7037(96)00236-0

Pälike, H., Lyle, M., Nishi, H., Raffi, I., Gamage, K., Klaus, A., and the Expedition 320/321 Scientists, 2010. *Proc. IODP,* 320/321: Washington, DC (Integrated Ocean Drilling Program Management International, Inc.). doi:10.2204/iodp.proc.320321.2010

Revillon, S., Barr, S., Brewer, T., Harvey, P., and Tarney, J., 2002. An alternative approach using integrated gamma-ray and geochemical data to estimate the inputs to subduction zones from ODP Leg 185, Site 801. *Geochem. Geophys. Geosyst.*, 3(12):8902. doi:10.1029/2002GC000344

Rudnick, R. L., and Gao, S., 2003. Composition of the continental crust. *In* Rudnick, R.L. (Ed.), *Treatise on Geochemistry, vol. 3, The Crust.* Amsterdam (Elsevier), 1–64.

Sakamoto, T., Saito, S., Shimada, C., and Yamane, M., 2003. Core-log integration of natural gamma ray intensity to construct a 10-my continuous sedimentary record off Sanriku, Western Pacific Margin, ODP Sites 1150 and 1151. *Proc. ODP, Sci. Results,* 186: College Station, TX (Ocean Drilling Program).

Sambridge, M., and Mosegaard, K., 2002. Monte Carlo methods in geophysical inverse problems. *Rev. Geophys.*, 40(3):1–29. doi:10.1029/2000RG000089

Taylor, S. R., and McLennan, S. M., 1985. *The Continental Crust: Its Composition and Evolution. An Examination of the Geochemical Record Preserved in Sedimentary Rocks:* Oxford (Blackwell Scientific Publications, Inc.).

Vasiliev, M. A., Blum, P., Chubarian, G., Olsen, R., Bennight, C., Cobine, T., Fackler, D., et al., 2011. A new natural gamma radiation measurement system for marine sediment and rock analysis. *J. Applied Geophys.*, 75(3):455–463. doi:10.1016/j.jappgeo.2011.08.008

Williams, T. J., and Winckler, G., 2012. Characterization of natural gamma radioactivity and ^{230}Th in the top of the sediment column in the eastern equatorial Pacific [Paper presented at 2012 Fall Meeting, AGU, San Francisco, 3–7 December 2012]. Abstract PP22A-03.

Wilson, S. A., 1997. Data compilation for USGS reference material BHVO-2, Hawaiian Basalt: *U.S. Geol. Survey Open-File Rept*.

Ziegler, C. L., Murray, R. W., Hovan, S. A., and Rea, D. K., 2007. Resolving eolian, volcanogenic, and authigenic components in pelagic sediment from the Pacific Ocean. *Earth Planet. Sci. Lett.*, 254:416–432. doi:10.1016/j.epsl.2006.11.049

Authors

Ann G. Dunlea, and **Richard W. Murray**, Department of Earth and Environment, Boston University, Boston, MA 02066, U.S.A., e-mail: adunlea@bu.edu; rickm@bu.edu

Robert N. Harris, College of Earth, Ocean, and Atmospheric Sciences, Oregon State University, Corvallis, OR 97331, U.S.A., e-mail: rharris@coas.oregonstate.edu

Maxim A. Vasiliev, (Currently) Baker Hughes, Inc., Houston, TX 77073, U.S.A., e-mail: maxim.vasilyev@bakerhughes.com

Helen Evans, Lamont-Doherty Earth Observatory, Palisades, NY 10964, U.S.A., e-mail: helen@ldeo.columbia.edu

Arthur J. Spivack, and **Steven D'Hondt**, Graduate School of Oceanography, University of Rhode Island, Narragansett, RI 02882, U.S.A., e-mail: spivack@gso.uri.edu; dhondt@gso.uri.edu